PTEP

Prog. Theor. Exp. Phys. **2012**, 03C008 (11 pages)
DOI: 10.1093/ptep/pts043

Nuclear physics at the SCRIT electron scattering facility

Toshimi Suda[1,*], Tatsuya Adachi[1], Tatsuya Amagai[1], Akitomo Enokizono[2], Masahiro Hara[3], Toshitada Hori[3], Shin'ichi Ichikawa[3], Kazuyoshi Kurita[2], Takaya Miyamoto[1], Ryo Ogawara[2], Tetsuya Ohnishi[3], Yuuto Shimakura[2], Tadaaki Tamae[1], Mamoru Togasaki[2], Masanori Wakasugi[3], Shuo Wang[1], and Kayoko Yanagi[1]

[1]*Research Center for Electron Photon Science, Tohoku University, 1-2-1 Mikamine, Sendai 982-0826*
[2]*Department of Physics, Rikkyo University, Nishiikebukuro, Toshima, Tokyo 171-8501*
[3]*Nishina Center for Accelerator-Based Science, RIKEN, 2-1 Hirosawa, Wako, Saitama 351-0198*
*E-mail: suda@lns.tohoku.ac.jp

Received August 15, 2012; Accepted August 27, 2012; Published December 17, 2012

The SCRIT electron scattering facility is under construction at the RIKEN RI Beam Factory. This is the world's first facility dedicated to the study of the structure of short-lived nuclei by electron scattering, which has been a long-standing dream for nuclear physics. A novel Self-Confining RI Target (SCRIT) technique makes this challenging research possible. A series of test experiments using stable nuclei performed at this partially completed facility show that the collision luminosity between electron beam and target nucleus reaches 10^{27} cm^{-2} s^{-1}, which is required for an elastic electron scattering measurement to determine the charge density distribution of the target nucleus. The first electron scattering for unstable Sn isotopes will take place in the year 2014.

Subject Index Nuclear Physics at the SCRIT Electron Scattering Facility

1. Introduction

Electron scattering provides the most reliable structure information for atomic nuclei [1], and thus has consistently played a key role in nuclear structure studies. A well-known textbook-type example is the charge density distributions of stable nuclei determined by elastic electron scattering [2]. Charge density distribution provides the most precise knowledge about the spatial distributions of atomic nuclei. Ever since the Nobel-prize experiment by R. Hofstadter and his colleagues about a half-century ago [3,4], elastic electron scattering has remained the one and only way to determine the charge density distribution in a nucleus.

The advantages of electron scattering are due to the fact that the electron is a point-like particle, and probes nuclei through the well-understood electromagnetic interaction. Since the electron-scattering process of a nucleus is well described by quantum electrodynamics [1], extraction of internal structure information from experimental data is straightforward and precise. In addition, the electromagnetic interaction is weak enough that the electron probes the whole volume of a target nucleus without serious distortion. This is in sharp contrast to structure studies by hadron probes, whose sensitivity is restricted to be around the nuclear surface due to the strong interaction.

So far, electron scattering has been limited mainly to stable nuclei, where one can prepare their "thick" targets. To be exact, there are several examples of electron scattering for unstable nuclei,

such as ^{3}H, ^{14}C, etc. [2], whose lifetimes are reasonably long. For highly unstable nuclei, however, no electron scattering experiments have ever been tried. This is simply due to the lack of a target-forming technique for rarely produced short-lived nuclei.

In this paper, we describe the world's first electron scattering facility dedicated to structure studies of short-lived nuclei, and the physics opportunities to be pursued at this facility. A novel target-forming technique, which we have invented and demonstrated as feasible, makes electron scattering for short-lived nuclei possible. This facility will open a completely new research field in nuclear physics: the study of the internal structure of rarely produced short-lived nuclei.

2. Electron scattering and structure studies of short-lived nuclei

Should electron scattering become feasible for short-lived nuclei, elastic scattering will first be measured as in the case for stable nuclei. This is because the elastic cross section is the largest among the other scattering processes in the low momentum transfer region. One determines the charge density distribution of a target nucleus from the elastic cross section, which is one of the basic ground-state properties of the nucleus.

2.1. Elastic scattering and charge density distribution

The differential cross section of elastic electron scattering from a spinless nucleus under PWIA (Plane Wave Impulse Approximation) is given as

$$\frac{\mathrm{d}\sigma}{\mathrm{d}\Omega} = \frac{\mathrm{d}\sigma_{\mathrm{Mott}}}{\mathrm{d}\Omega}|F_{\mathrm{c}}(q)|^2, \tag{1}$$

where $\mathrm{d}\sigma_{\mathrm{Mott}}/\mathrm{d}\Omega$ is the Mott cross section, and $F_{\mathrm{c}}(q)$ the charge form factor. The momentum transfer, $\vec{q}$, is defined by incident and scattered electron momentum vectors, $\vec{e}$ and $\vec{e'}$, as,

$$\vec{q} = \vec{e} - \vec{e'}. \tag{2}$$

The Mott cross section is the elastic cross section from a point particle of charge Z,

$$\frac{\mathrm{d}\sigma_{\mathrm{Mott}}}{\mathrm{d}\Omega} = \frac{Z^2\alpha^2}{4E_{\mathrm{e}}^2}\frac{\cos^2(\frac{\theta}{2})}{\sin^4(\frac{\theta}{2})}, \tag{3}$$

where E_{e} is the electron energy, θ the scattering angle, and α the fine-structure constant, respectively. The form factor is a Fourier component of the charge density distribution, $\rho_{\mathrm{c}}(r)$, for the momentum transfer $\vec{q}$,

$$F_{\mathrm{c}}(q) = \int \rho_{\mathrm{c}}(r)\mathrm{e}^{\mathrm{i}\vec{q}\cdot\vec{r}}\mathrm{d}\vec{r}. \tag{4}$$

One can, thus, determine $\rho_{\mathrm{c}}(r)$ for a target nucleus from the elastic cross section measured as a function of the momentum transfer $\vec{q}$. For most stable nuclei, a complete data set of the form factors measured up to the high momentum transfer region is available [2].

For rarely produced short-lived nuclei, the anticipated low luminosities may limit the accessible momentum transfer, since the elastic cross section decreases as $\sim 1/q^4$. The measurement in a limited momentum transfer range may reveal only gross features of the charge distribution, such as the radius and surface diffuseness. Despite this limitation, those radial properties along the isotopic chains would certainly be very important, and would be an essential basis for any nuclear structure models applicable to short-lived nuclei.

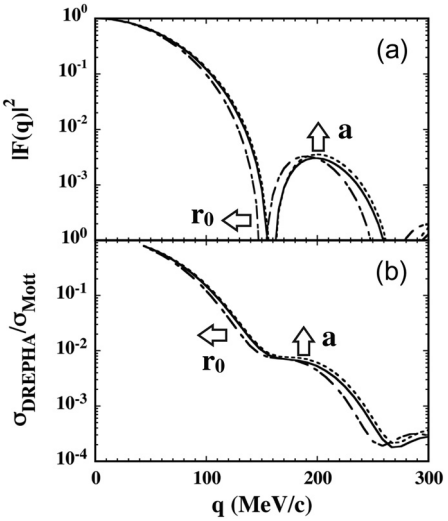

Fig. 1. Charge form factor for Sn assuming the two-parameter Fermi type distribution. (a) The parameters for the size and surface diffuseness are changed by −5% and −10%. (b) The result of a distorted-wave calculation divided by the Mott cross section, corresponding to the charge form factor in the PWIA treatment.

Figure 1 shows the results of calculations for the charge form factor of Sn, whose atomic number is $Z = 50$. A two-parameter Fermi distribution, a typical profile of stable nuclei, is assumed in the calculation,

$$\rho(r) = \frac{\rho_0}{1 + \exp(\frac{r - r_0}{a})}. \tag{5}$$

The results of modifying the parameters for the diffraction radius, r_0, by −5% and the surface diffuseness, a, by −10% are plotted in Fig. 1(a). It should be noted that the dip position and the height of the diffraction maxima are separately sensitive to the change in size and diffuseness. The form factor measurement covering the first maximum will, thus, determine the (diffraction) radius and the surface diffuseness.

In reality, the PWIA framework is known to be inadequate for medium and heavy nuclei, such as Sn isotopes, because of the serious distortion effects for the incoming and outgoing electron waves in the Coulomb fields of the nucleus. One must carry out a distorted wave calculation to treat the distortion effects. Figure 1(b) shows the results of one such distorted wave calculation code, DREPHA (B. Dreher and J. Friedrich, *DREPHA: A phase-shift calculation code for elastic electron scattering*, private communication). The calculated cross section is divided by the Mott cross section, $\sigma_{\mathrm{DREPHA}}/\sigma_{\mathrm{Mott}}$, which corresponds to the form factor squared in the PWIA framework. Similar sensitivities of the elastic cross section to changes of radius and surface diffuseness were confirmed by the distorted wave calculation.

2.2. Day One experiment: The charge density distribution of unstable Sn isotopes

The first experiment at this new facility will be for unstable Sn isotopes including ^{132}Sn. The ^{132}Sn nucleus is a doubly magic nucleus whose life time is 40 seconds.

The Sn nucleus has the largest number of *stable* isotopes among the elements, i.e. ^{112}Sn–^{124}Sn, whose charge density distributions have already been determined precisely by elastic electron scattering [2]. Extending the target Sn isotopes to unstable ones, ^{126}Sn–^{132}Sn, we will study how the charge distributions, i.e. radius and surface diffuseness, change along the isotopic chain over 20 additional

neutrons, ^{112}Sn–^{132}Sn. Precise measurements about how the charge density distributions change as a function of the neutron number will shed light on the isospin-dependent term of the potential.

According to simulations using the DREPHA code, a luminosity of at least 1×10^{27} cm^{-2} s^{-1} is needed to determine the size and the diffuseness with an accuracy better than a few per cent within a reasonable measuring time of one week.

3. SCRIT

A way to make this challenging research possible is to utilize a novel experimental technique we invented, which we named SCRIT (Self-Confining RI Target) [5]. It is inspired by the well-known ion trapping phenomenon observed at electron storage ring facilities. The residual gases in a storage ring are ionized by the circulating electron beam. Once they are ionized, they are trapped transversely by the electron beam. Since the trapped ions stay on the electron beam and kick electrons out of orbit, the results of this ion trapping are harmful for the performance of electron storage rings. This leads to shorter beam lifetime, and even beam instability when the trapping becomes severe. Thus, much effort has been paid so far to reducing the negative effects of ion trapping [6].

SCRIT uses the ion trapping in a positive way to form a target of short-lived nuclei, as trapped ions, on the electron beam. The ions of short-lived nuclei produced at an external ion source are transported to the electron storage ring, and are kept on the electron beam by the ion-trapping phenomena. Placing a longitudinal mirror potential along the electron beam line, one can form a three-dimensionally localized target on the electron beam. By controlling the voltage applied to the electrodes for the mirror potential, one can easily control ion injection and ejection, and thereby the ion-trapping period, which is essential for targeting short-lived nuclei.

3.1. A proof-of-principle study

In order to study the feasibility of this new scheme, a proof-of-principle experiment using a prototype device was conducted at the electron storage ring of Kyoto University, KSR [7]. A stable nucleus, ^{133}Cs, was employed as a target. The electron beam energy, typical stored beam current and the beam lifetime were 120 MeV, 75 mA and 100 seconds, respectively.

The prototype device consists of an external Cs ion source, electrodes for forming the mirror potential, an ion analyzer for monitoring the trapped Cs ions, and an electron detector, each of which were in a vacuum except for the electron detectors, which consisted of a drift chamber and calorimeters [8].

At an average electron beam current of 75 mA, we measured the scattered electrons from the trapped Cs ions with the ion injection–trap–ejection cycle, whose trapping time was set to 50 ms to simulate short-lived nuclei. Elastically scattered electrons from the trapped Cs ions were clearly observed. Using the known elastic scattering cross section, the luminosity of 1×10^{26} cm^{-2} s^{-1} was deduced at the average electron beam current of 75 mA with 10^6 trapped ions [9].

4. The SCRIT electron scattering facility

Based on the success of the SCRIT feasibility studies, we have started the construction of the world's first electron scattering facility with the SCRIT system in the RIKEN RI Beam Factory.

4.1. Facility overview

Figure 2 shows the layout of the SCRIT electron scattering facility. The details of the facility will be described elsewhere (a paper on the SCRIT electron facility, in preparation). It consists of an

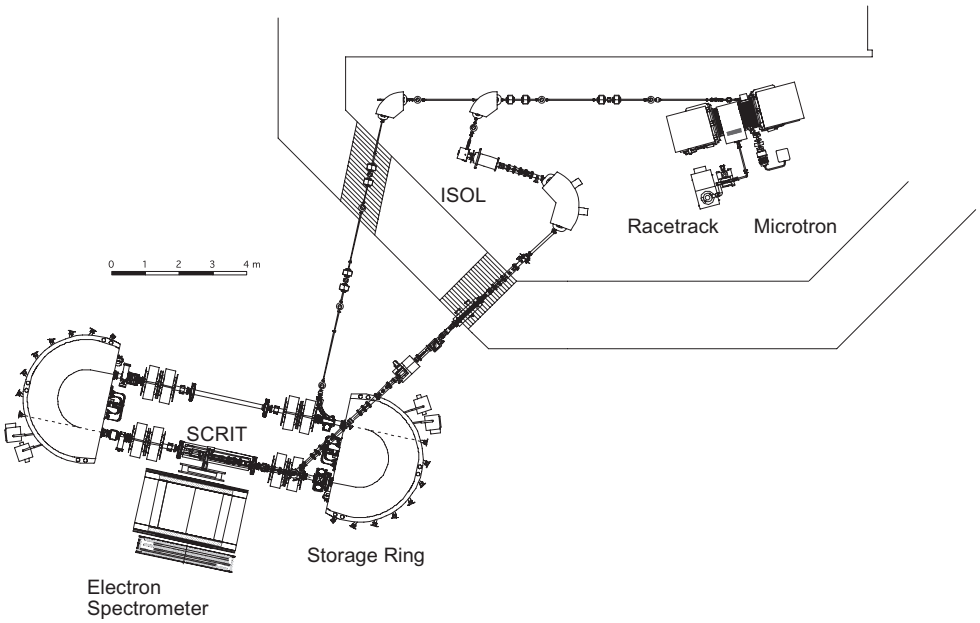

Fig. 2. The SCRIT electron scattering facility.

electron accelerator with the SCRIT system, an ISOL (Isotope Separator On-Line) system and an electron spectrometer system.

The construction of the electron accelerator with the SCRIT system has been completed and is already commissioned. Today, the construction of the ISOL and the electron spectrometer is under way.

The electron accelerator consists of a 150-MeV injector racetrack microtron and a 700-MeV electron storage ring. The stored electron beam energy is variable from 150 MeV to 700 MeV. The basic configuration of the electron ring is the same as that of the SR light source facility, HiSOR [10,11], of Hiroshima University. The pulsed 150-MeV electron beam with a peak current of 0.5 mA and a pulse width of 1 μs is injected with a repetition rate of 2 Hz to fill the ring. The stored beam current today is over 250 mA, with a beam lifetime of over 200 minutes.

An ISOL system to produce neutron-rich nuclei via the photo-fission process of uranium is under construction. The long beam lifetime of the stored electron beam, a few hours, enables us to use the microtron as a driver for the ISOL. This ISOL system makes it possible to operate the facility completely independently of the other facilities of the RI Beam Factory.

4.2. The SCRIT system

Figure 3 shows the SCRIT system installed in the straight section of the storage ring. The system consists of a set of deflectors for ion injection and ejection, three electrodes and a trapped-ion analyzer. Two sets of beam scrapers and two sets of button-type beam position monitors (BPMs) are installed along the electron (and ion) beam line. They are all on a movable platform for fine position tuning.

The electrodes are racetrack in shape. The electrodes at both ends provide a mirror potential to keep ions longitudinally inside the SCRIT device, and the centeral electrode with a length of 500 mm is to trap ions with a kinetic energy of the order of a few eV.

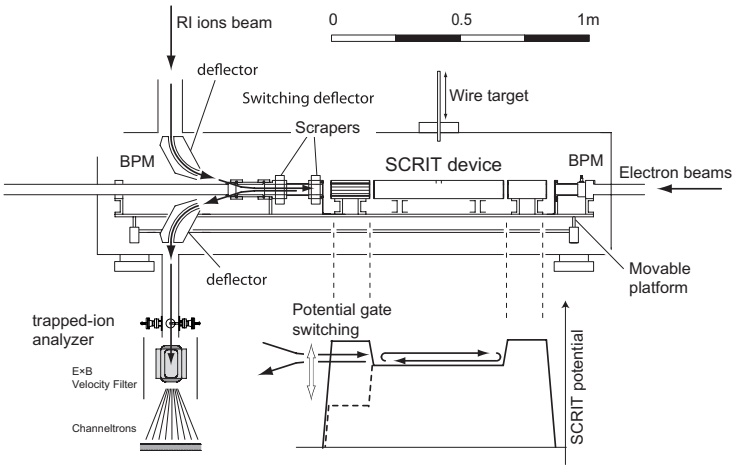

Fig. 3. The SCRIT device.

The pulsed ion beam from an external ion source is transported through the deflector and then merged with the stored electron beam. As shown in Fig. 3, the ions are introduced inside the mirror potential by controlling the voltage of the entrance electrode. After a certain trapping time determined by the lifetime of the short-lived nuclei to maintain target purity, they are ejected from the potential and guided to the trapped-ion analyzer, where the charge state of the trapped ions is measured. The change of their charge state is a good measure of the spatial overlap between the electron beam and the trapped ions. Better spatial overlap, providing higher luminosity, results in higher-charge-state Cs ions due to further ionization of the trapped ions by the electron beam.

4.3. ISOL

Production of short-lived nuclei will be carried out using the 150-MeV electron beam from the microtron bombarding a uranium carbide target, $^{238}UC_x$. Photo-fission (and electro-fission) of uranium is known to be an efficient way to produce medium-heavy neutron-rich nuclei such as Sn isotopes, especially ^{132}Sn [12].

Photo-fission of uranium is mainly induced by the excitation of the giant dipole resonance of ^{238}U at $E_\gamma \sim 15$ MeV. In the $^{238}UC_x$ target, the incident energy of the electron beam is immediately shared by lots of γ, e^-, and e^+ created in electromagnetic-shower processes. GEANT simulations show that the photo-fission rate per unit beam power for the optimized target geometry does not strongly depend on the incident electron energy. For incident electron energy higher than 100 MeV, the fission rate is nearly constant: of the order of 10^8 fissions per watt.

In order to strengthen the beam power up to 1 kW, which provides a 10^{11} s^{-1} fission rate, an upgrade of the microtron will be carried out at a higher repetition rate of 150 Hz with a wider pulse width of 10 μs. Since the average yield of ^{132}Sn in the photo-fission process is known to be around 1% [12], the production rate of ^{132}Sn is expected to be about 10^9 s^{-1}.

4.4. Electron spectrometer

An electron spectrometer, whose momentum resolution is $\Delta p/p \sim 1 \times 10^{-3}$, is under construction. In consideration of the momentum transfer range required to measure diffraction patterns of the elastic cross section, the electron beam energy should be in the range of 150–300 MeV. The energy resolution of this spectrometer system will thus be a few 100 keV.

Due to the fact that the SCRIT provides a spatially extended target, ∼500 mm, along the electron beam, we employ a non-focusing-type spectrometer. The trajectories of the scattered electrons are measured with drift chambers placed at both the entrance and exit of the magnet.

The spectrometer will have a wide coverage of the scattering angle for precise measurements of momentum-transfer dependence of the elastic cross section. Employing an H-type dipole magnet having a rectangular shape, whose gap is 170 cm (width) × 29 cm (height) × 140 cm (length), a wide angular coverage of 30–60 degrees is realized with a solid angle of 100 msr. The magnetic field is 0.8 T for 300 MeV electrons. The momentum transfer region for elastic scattering will be from 80 MeV/c at $E_e = 150$ MeV to 300 MeV/c at $E_e = 300$ MeV.

The OPERA-3D calculations [13] show that inhomogeneity of the magnetic field over the entire gap volume is less than 0.2%. Two field-cramps were installed at each end to minimize the field leakage at the position of the circulating electron beam. This leakage is expected to be less than 5 gauss, and is unlikely to affect the electron beam orbit seriously.

5. Performance studies of the facility

A series of test experiments have been conducted to study the SCRIT facility's performance as an electron scattering facility for short-lived nuclei. The primary purpose was to study the achievable luminosity at the new facility. The electron beam energy for this series of studies was fixed at 150 MeV, and stable Cs and Xe ions were used as targets.

5.1. Study using Cs ions

The first study immediately after the accelerator commissioning was conducted using stable ^{133}Cs ions. An ion source of the surface-ionization type used in the KSR study was attached to a temporarily built ion-beam transport line. A pulsed Cs^{1+} ion beam with a pulse width of 300 μs and kinetic energy of 6.05 kV was transported to the SCRIT system. Optimization of the spatial overlap between the electron beam and the injected Cs ions was done in two ways. One was to analyze the charge state of the trapped ions using the ion analyzer, and the other was to detect events by a pair of plastic scintillators originated from elastically scattered electrons at an ultra-forward angle, where the elastic cross section is huge.

Ion-trapping cycles were repeated at a frequency of 20 Hz at a storage beam current of about 200 mA. In order to mimic a target with short-lived nuclei, the trapping time was set to 45 ms. The Cs ions were injected every two cycles by controlling the grid of the ion source for repetitive measurements of the scattered electrons under conditions both with and without the trapped Cs ions.

For precise luminosity determination, we measured the elastically scattered electrons from the trapped Cs ions. The scattered electrons were detected by a drift chamber and a pure CsI calorimeter as in the KSR study [9]. The precise scattering angle and reaction vertices were determined from the electron trajectories measured by the drift chamber. Knowing the electron energy measured by the calorimeter, elastic events from the trapped Cs ions could be identified. Since the elastic cross section is known, one can determine the achieved luminosity.

Figure 4 shows the vertex distribution of the detected electrons with and without the trapped Cs ions. Here, electrons whose energies were over 100 MeV were used for this plot. A clear enhancement due to the trapped Cs ions was seen in the vertex distribution, which is consistent with the ion-trap region set by the electrodes. The sharp peaks observed at −350 mm, −150 mm, and 400 mm were attributed to beam halos hitting the thick terminal electrodes. The upper panel in Fig. 4 shows the vertex distribution where the contribution from the Cs-off measurement is subtracted. Electrons from

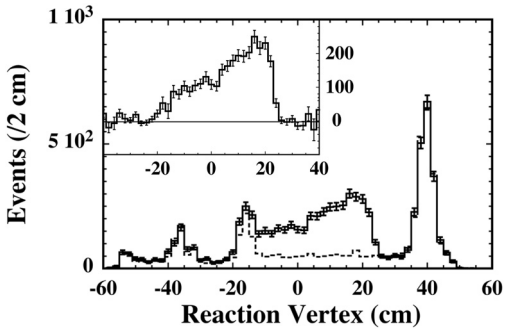

Fig. 4. Electron vertex distribution. Solid (dashed) lines show the distributions measured with (without) trapped Cs ions. The scattered electrons whose energies are larger than 100 MeV are selected. The upper panel shows the subtracted vertex distribution.

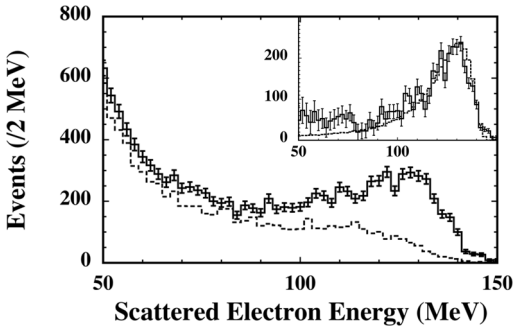

Fig. 5. Scattered electron energy spectrum, whose vertices are in the trapped region. Solid (dashed) lines show the distributions measured with (without) trapped Cs ions. The upper panel shows the subtracted energy spectrum with the detector response for $E_e = 150$ MeV simulated by GEANT.

only the trap region are seen, and the beam halo contribution disappears. The vertex dependence is found to be consistent with the angular dependence of the elastic cross section for Cs.

Figure 5 shows the energy spectra of the detected electrons with and without the trapped Cs ions. Note that their vertices are limited in the trapping region. The spectrum shape of the subtracted events, shown in the upper panel in Fig. 5, is consistent with the detector response simulated by GEANT for 150 MeV electrons. Thus, they are concluded to be those from elastic scattering. It should be noted here that a contribution from inelastic scattering is safely neglected under these kinematics.

Detailed analysis including a Distorted Wave Born Approximation (DWBA) calculation using DREPHA code concluded that the absolute luminosity achieved was $9 \times 10^{26}\,\mathrm{cm}^{-2}\,\mathrm{s}^{-1}$. The number of injected Cs ions was $2 \times 10^{9}\,\mathrm{s}^{-1}$ on average, and 10% of them were found to contribute to the collision luminosity.

This is indeed the luminosity required for elastic scattering for short-lived nuclei. We thus concluded that elastic electron scattering experiments for short-lived nuclei are feasible at the SCRIT electron scattering facility. Further details, including the time evolution of the trapped ions, together with the instantaneous variation of the luminosity, will soon be published elsewhere (a paper on the SCRIT electron facility, in preparation).

5.2. Study using Xe ions

A new ion beam transport line connecting the ISOL and the SCRIT device was completed in FY2012. An ion-trapping study with Xe ions instead of Cs is under way. Natural Xe gas includes nine stable

Xe isotopes, which enables us to check the performance of the new ion transport line, such as the mass resolution.

An identical ion-trapping sequence to that for Cs ions is employed for the achievable luminosity study. The first measurement of elastically scattered electrons from the trapped Xe ions was successful: so far, a luminosity of $3 \times 10^{26}\,\mathrm{cm}^{-2}\,\mathrm{s}^{-1}$ has been achieved. Further optimization, including the operation of the new ion transport line, is under way to achieve higher luminosity.

6. Nuclear physics at the SCRIT electron scattering facility

The SCRIT electron scattering facility will be the world's first and only facility of its type. Since structure studies of short-lived nuclei by electron scattering have been a long-standing dream, the impact of the research to be performed at this facility will be quite strong for nuclear physics.

As discussed previously, the Day One experiment will be the measurement of the elastic scattering cross section for the unstable Sn isotopes, including the doubly magic ^{132}Sn. What follows is a list of additional research opportunities currently being discussed.

6.1. Elastic scattering

It is straightforward to extend the elastic scattering experiments to other short-lived nuclei once the elements are available from the ISOL system. A series of experiments for many elements along the isotopic chain will provide essential inputs for any sophisticated nuclear structure models.

One good example are the Ar isotopes. A peculiar "bubble" structure in the charge density distribution is suggested in ^{46}Ar [14]. It is pointed out that an inversion of the 1/2 state with the state usually located above is expected in the neutron-rich Ar isotopes. Elastic electron scattering will be the only way to quantify this peculiar structure.

6.2. Beyond elastic scattering

As the luminosity is improved, studies beyond elastic scattering will come into our sights. For instance, the measurement of inelastic scattering becomes possible for luminosity of $\sim 10^{28-29}\,\mathrm{cm}^{-2}\mathrm{s}^{-1}$. One can determine the transition density of a specific excitation level, from which one obtains fruitful information on the wave function of the excitation level as demonstrated for stable nuclei [15].

At even higher luminosity, of the order of $\sim 10^{29-30}\,\mathrm{cm}^{-2}\,\mathrm{s}^{-1}$, it would be possible to carry out coincidence experiments, $(e, e'p)$, in the quasi-elastic kinematics, which is known to be the most powerful tool for studying the single nucleon properties of a nucleus. Good examples are the single particle momentum density distributions of many stable nuclei [16]. The spectroscopic factor of the bound protons in a specific orbit is also deduced from the quasi-elastic $(e, e'p)$ data [17]. They provide a stringent testing ground of nuclear structure theory. Since the quasi-elastic $(e, e'p)$ is much cleaner and superior to other hadron-involved reactions for spectroscopic study, we would like to make much effort to improve the luminosity to go beyond elastic scattering in the future.

6.3. Photonuclear reaction

Recently, a new research possibility at the SCRIT electron scattering facility was pointed out: the measurement of the total photoabsorption cross section of short-lived nuclei.

It is well known that the inelastic electron scattering cross section at the forward angle, $\theta \sim 0$, offers the same information as nuclear excitation by real photons [18,19]. We intend to measure the

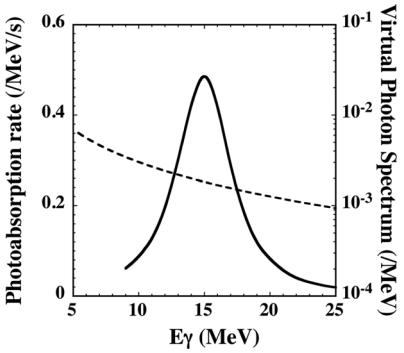

Fig. 6. The expected photo absorption rate in the giant dipole resonance region of Sn isotope (solid line) at a luminosity of $1 \times 10^{27}\,\mathrm{cm}^{-2}\,\mathrm{s}^{-1}$, and the calculated virtual photon spectrum (dashed line). The total photo absorption cross section for ^{124}Sn [20] is used.

inelastic cross section at the forward angle to determine the photonuclear response of short-lived nuclei in the photon energy range from a few MeV to 40 MeV to cover the giant dipole resonance. Assuming a luminosity of $10^{27}\,\mathrm{cm}^{-2}\,\mathrm{s}^{-1}$, the estimated counting rate of photonuclear reaction for Sn isotopes in the giant dipole resonance region is shown in Fig. 6. The measured photo absorption cross section for ^{124}Sn [20] is used for the estimation, and the virtual photon theory by Onley [21] is employed to calculate the virtual photon spectrum.

Inelastically scattered electrons at extremely forward angles will be momentum-analyzed and detected in the bending magnet of the storage ring in coincidence with nuclear reaction products such as neutrons. A feasibility study for detecting lower-energy electrons inside the dipole magnet has already been initiated.

7. Conclusions

The SCRIT electron scattering facility will open a completely new research field in nuclear physics: structure studies of short-lived nuclei by electron scattering.

The construction of the electron accelerators equipped with the SCRIT system and the ion-transport line have been completed, and are already commissioned. The results of performance studies using stable Cs and Xe ions as trapped targets at the SCRIT system are promising. The luminosity required for elastic electron scattering, $\sim 10^{27}\mathrm{cm}^{-2}\,\mathrm{s}^{-1}$, is achieved with the order of 10^7 trapped ions.

An electron spectrometer having a momentum resolution of $\Delta p/p = 10^{-3}$ and an ISOL system for producing neutron-rich short-lived nuclei via electro- (photo-) fission of uranium are both under construction, and they are well on track. The Day One experiment will be elastic electron scattering for short-lived Sn isotopes, including the doubly-magic nuclei ^{132}Sn, in the year 2014.

Acknowledgment

This work is supported by Grants-in-Aid for Scientific Research (S) (Grants No. 22224004), Grants-in-Aid for Scientific Research (B) (Grants No. 24340057) from JSPS, and Rikkyo SFR, Joint Research Project(2005-06).

References

[1] T. deForest Jr. and J.D. Walecka, Adv. in Phys. **5**, 1 (1966).
[2] H. deVries, C.W. deJager, and C. deVries, At. Data Nucl. Data Tables **36**, 495 (1987).
[3] B. Hahn, D.G. Ravenhall, and R. Hofstadter, Phys. Rev. **101**, 1131 (1956).

[4] R. Hofstadter, *Nobel Lecture: The Electron-Scattering Method and its Application to the Structure of Nuclei and Nucleons* (Nobelprize.org, 1961). (Available at http://www.nobelprize.org/nobel_prizes/physics/laureates/1961/hofstadter-lecture.html, date last accessed: October 17, 2012.)
[5] M. Wakasugi, T. Suda, and Y. Yano, Nucl. Instrum. Methods A **532**, 216 (2004).
[6] C.J. Bocchetta and A. Wrulich, Nucl. Instrum. Methods A **278**, 807 (1989).
[7] A. Noda, Proc. 5th European Particle Accelerator Conf., Barcelona, p. 451 (1996).
[8] M. Wakasugi, T. Emoto, Y. Furukawa, K. Ishii, S. Ito, T. Koseki, K. Kurita, A. Kuwajima, T. Masuda, A. Morikawa, M. Nakamura, A. Noda, T. Ohnishi, T. Shirai, T. Suda, H. Takeda, T. Tamae, H. Tongu, S. Wang, and Y. Yano, Phys. Rev. Lett. **100**, 164801 (2008).
[9] T. Suda, M. Wakasugi, T. Emoto, K. Ishii, S. Ito, K. Kurita, A. Kuwajima, A. Noda, T. Shirai, T. Tamae, H. Tongu, S. Wang, and Y. Yano, Phys. Rev. Lett. **102**, 102501 (2009).
[10] K. Yoshida, M. Andreyashkin, K. Goto, G. Kutluk, K. Matsui, K. Miura, H. Namatame, N. Ojima, K. Shimada, M. Taniguchi, S. Yagi, I. Endo, T. Takahashi, A. Hiraya, H. Sato, T. Sekitani, K. Tanaka, H. Yoshida, D. Amano, K. Aoki, T. Hori, K. Kawamura, T. Takayama, N. Yasumitsu, T. Ishizuka, H. Morimoto, Proc. APAC98, p. 653 (1998).
[11] T. Hori, J. Yang, and M. Washio, Proc. EPAC98, Stockholm, p. 517 (1998).
[12] D. De Frenne, H. Thierens, B. Proot, E. Jacobs, P. De Gelder, and A. De Clercq, Phys. Rev. C **29**, 1908 (1984).
[13] *TOSCA*, Vector Fields Ltd, Oxford, England.
[14] E. Khan, M. Grasso, J. Margueron, and N. Van Giai, Nucl. Phys. A **800**, 37 (2008).
[15] H.P. Blok and J.H. Heisenberg, High Resolution Inelastic Electron Scattering and Nuclear Structure. In *Modern Topics in Electron Scattering*, eds. B. Frois and I. Sick (World Scientific, Singapore, 1991) p. 393.
[16] P.K.A. de Witt Huberts, J. Phys. G: Nucl. Part. Phys. **16**, 507 (1990).
[17] G.J. Kramer, H.P. Blok, and L. Lapikas, Nucl. Phys. A **679**, 267 (2001).
[18] C.A. Bertulani, Phys. Rev. C **75**, 024606 (2007).
[19] I.C. Nascimento, E. Wolynec, and D.S. Onley, Nucl. Phys. A **246**, 210 (1975).
[20] B.L. Berman and S.C. Fultz, Rev. Mod. Phys. **47**, 713 (1975).
[21] P. Durgapal, D.S. Onley, Comp, Phys, Commun. **32**, 291 (1984).